Effects of EDTA on adsorption of Cd(II) and Pb(II) by low-permeability soil minerals and on their microscopic characteristics

Xueji You
Tongji University
Shuguang Liu
Tongji University
Chaomeng Dai (daichaomeng@tongji.edu.cn)
Tongji University https://orcid.org/0000-0003-1567-8212
Guihui Zhong
Tongji University
Yanping Duan
Shanghai Normal University
Yiping Guo
McMaster University
Aleksei Nikolavich Makhinov
Far East Branch of the Russian Academy of Sciences
José Tavares Araruna Júnior
Pontifical Catholic University of Rio de Janeiro
Yaojen Tu
Shanghai Normal University
Kah Hon Leong
Universiti Tunku Abdul Rahman

Research

Keywords: Low-permeability, Adsorption capacity, Cadmium, Lead, Soil minerals, Clay, Low-molecular-weight organic acids

Posted Date: January 3rd, 2020

DOI: https://doi.org/10.21203/rs.2.19991/v1

Abstract

Background

Ethylenediaminetetraacetic acid (EDTA) can serve as a washing agent in the remediation of low-permeability layers contaminated by heavy metals (HMs). Therefore, batch adsorption experiments, where quartz sands (SM1) and mineral mixtures (SM2) were used as low-permeability soil minerals (SMs), were implemented to explore the effects of different EDTA concentrations, pH and exogenous chemicals on the HM-SM-EDTA adsorption system. Changes in microscopic characterizes of SMs were determined by instrument analysis to investigate the mechanisms.

Results

As the EDTA concentration increased gradually, it gradually cut down the maximum Cd adsorption capacities of SM1 and SM2 from approximately 135 to 55 mg/kg and 2,660 to 1,453 mg/kg; and the maximum Pb adsorption capacities of SM1 and SM2 were reduced from 660 to 306 mg/kg and 19,677 to 19,262 mg/kg, respectively. When the mole ratio (MR = moles of HM ions / sum of moles of HM ions and EDTA) was closer to 0.5, the effect of EDTA was more effective; and Freundlich isotherm model fitted better to the data. It took 5 to 10 min for EDTA to begin taking its effect. EDTA worked well at pH below 7.0 and 4.0 for Cd and Pb, respectively. Low-molecular-weight organic acids (LMWOAs) affected the system mainly by bridging, complexation, adsorption site competition and reductive dissolution. Cu^{2+}, Fe^{2+} ions could greatly increase the Cd and Pb adsorption on SM2. There were feature changes in mineral particles including attachment of EDTA and microparticles, agglomeration, connection and smoother surfaces, making the specific surface area decrease from 16.73 to 12.59 m^2/g.

Conclusion

All findings indicated that EDTA could effectively and economically reduce the HM adsorption capacity of SMs at the reasonable MR value, contact time and pH. The extent of the effects of LMWOAs and exogenous metal ions on the HM-SM-EDTA system depended on the synthesis of diverse effects and the selectivity of EDTA, respectively. EDTA reduced the HM adsorption capacity of SMs not only by complexation with HM ions, but also decreasing SSA and blocking active sites. Hence, the acquired insight from the presented study can help to promote the remediation of contaminated soil and groundwater.

1 Background

Sanitary wastewater, agricultural and industrial discharges from increasing human activities has made heavy metal pollution become a ubiquitous environmental problem, especially in soil and groundwater system [1–4]. Enriched heavy metals (HMs) in the environment seriously threaten the ecological system and human health due to high toxicity, the nonbiodegradable nature and the ability of retention [4–6]. Toxic metals such as lead (Pb(II)), chromium (Cr(VI)), nickel (Ni(II)) and cadmium (Cd(II)) can cause many

severe health effects including bone fractures, organ disorders and brain damage [7]. Specifically, lead can be toxic to lives even at low concentrations [8]; cadmium can increase the risk of cancer [3, 9–10]. Therefore, many water treatment technologies, such as membrane filtration [11], precipitation [12], electrodialysis [13] and so on, are developed to try to completely remove HMs from wastewaters before discharging.

However, there are usually some low-permeability layers in the soil and groundwater environment, which can act as principal obstacles to retard pollutant migration and serve as pollution sinks to store pollutants due to their strong adsorption capability and special diffusion properties [14–17]. On the one hand, because of their low hydraulic conductivity, water flow and solute transport in low-permeability layers are slow [18]. On the other hand, low-permeability layers mainly consist of low-permeability soil minerals such as silt and clay [19]; note that these minerals have great affinity and selectivity to HMs, especially clay [20–23]. As a result, a large quantity of HMs from wastewater has accumulated in the soil and groundwater system since long time ago, which enhances the hazards of heavy metal pollution and is also quite difficult to restore. Specifically, low-permeability layers serve as long-term reservoirs for pollutants, simultaneously, it also become a secondary pollutant source and constantly release pollution by back-diffusion [16, 18, 24]; this would greatly extend the timeframe and difficulty of remediation.

Naturally, many technologies have been put forward to restore the low-permeability layers contaminated by HMs, which are mainly divided into physical, chemical, and biological methods. And soil washing combined with pump-and-treat remediation is relatively effective and economic [1]. Considering the strong adsorption capability of low-permeability soil minerals for HMs, ethylenediaminetetraacetic acid (EDTA), a chelating agent, are commonly serve as a washing agent [25–26]; because it can form strong negatively charged complexes with divalent metal cations in solution through its two amines and four carboxylate groups, improve the mobility of HMs, and reduce HM adsorption on low-permeability soil minerals [27–29]. Consequently, the amount of synthetic EDTA in the environment is constantly increasing, such as an average annual rate of 8% in China[25]. Necessarily, this study tried to determine the reasonable condition for EDTA to reducing the HM adsorption on low-permeability soil minerals, and investigate the effects of EDTA on the minerals; so that the remediation technology can be refined and promoted.

Within the range of relevant natural conditions, the process of Cd and Pb adsorption onto soil minerals (SMs) was simulated by batch adsorption experiments. The objectives of this study were as follow: (a) to investigate the effects of EDTA on adsorption of Cd and Pb by low-permeability soil minerals, analyze the adsorption isotherm and kinetics, and clarify the basic behavior of the HM-SM-EDTA system; (b) to examine the influences of contact time, pH and exogenous chemicals (low-molecular-weight organic acids (LMWOAs) and exogenous metal ions) on the HM-SM-EDTA system, and determine the reasonable conditions for EDTA to work effectively and economically; and (c) to analyze changes in microscopic characteristics of soil minerals under the effects of EDTA, and study the mechanisms.

2 Materials And Methods

2.1 Selection of soil minerals and chemicals

To simulate commonly media such as silt and clay in low-permeability layers [18, 24, 30], two types of soil minerals (SMs), fine quartz sands (SM1) and the mineral mixtures of quartz sands and clay (SM2), were typically used in the experiments; and they both had a medium grain size of 50 μm and represented unreactive and reactive minerals for contrast. Fine quartz sands served as the control group to investigate the basic adsorption phenomenon. To cover typical clay minerals in natural low-permeability layers, SM2 were comprised of 50-μm fine quartz sand, illite and montmorillonite (Junhong New Material Co., Ltd., Shanxi, China) at a mass ratio of 1:1:1 [31–32].

All of the chemicals required for the experiments were of analytical grade or higher and used without further purification. Ethylenediaminetetraacetic acid disodium salt (EDTA-2Na), cadmium chloride ($CdCl_2$, 99%), and lead chloride ($PbCl_2$, 99.5%) were purchased from Sinopharm Chemical Reagent Co., Ltd. (China); All low molecular weight organic acids (LMWOAs, including Acetic acid, 99.5%; Ascorbic acid, > 99.0%; Citric acid, ≥ 99.5%; Oxalic acid, ≥ 99.5%; Malonic acid, 99.5%; Succinic acid, 99.5%; Tartaric acid, 99%; and Humic acid), and other metal chlorides ($CuCl_2{\cdot}2H_2O$, $MnCl_2{\cdot}4H_2O$, $CrCl_3{\cdot}6H_2O$, $FeCl_2{\cdot}4H_2O$, $MgCl_2{\cdot}6H_2O$, $AlCl_3{\cdot}6H_2O$) were obtained from Shanghai Macklin Biochemical Co., Ltd. (China). Deionized water (18.2 MΩ cm) mentioned in this study was obtained by a Milli-Q ultrapure water purification system (Ultrapure Corp., CA, USA).

2.2 Batch adsorption experiments

The effects of EDTA-2Na on heavy metal (HM) adsorption by soil minerals were systematically studied by utilizing Cd(II) and Pb(II) as analytes; batch adsorption experiments were carried out on an incubator shaker at 250 rpm in 50-mL tubes containing 2.4 g soil minerals and 25 mL solution of heavy metal ions, which was the HM-SM system. To explore the effects of EDTA, different doses of EDTA-2Na were added into the above system; and this formed the HM-SM-EDTA system. To investigate the isotherms model, the adsorption experiments were performed at Cd and Pb concentration vary from 10 to 400 mg/L and 10 to 2000 mg/L, respectively. For the kinetic study, the samples were withdrawn at fixed intervals (2, 5, 10, 20, 30, 60, 100, 180, and 360 min). The effect of pH values (2.0–12.0) on the HM-SM-EDTA system was investigated by adjusting the initial pH of the solution mixture by either HCl or NaOH solutions (1.0 mol/L). Low-molecular-weight organic acids and exogenous metal ions were all introduced into this system with a concentration of 0.001 M to explore their effects. The concentrations of Cd, Pb, and EDTA-2Na, pH, contact time, and temperature in the batch experiments were 200, 300, and 400 mg/L, 5.5, 360 min, and 25 ℃, except where the concentration, pH, contact time, and temperature were controlling factors as described above. After adsorption, soil minerals were separated by centrifugation at 3000 rpm for 10 min; the supernatants were collected and filtered through 0.22-μm filter membranes. Then, the heavy metal concentrations were analyzed by an inductively coupled plasma optical emission spectrometer (720ES, Agilent Technologies, Inc., USA); and the soil minerals were prepared by vacuum freeze drying for use in analytical instrument tests. Three replicates were conducted for each adsorption

experiment and the mean values were reported. Adsorption capacities (q_t, mg/g) were calculated as the following Eq. (1):

$$q_t = \frac{C_0 - C_t}{m} V \quad (1)$$

where C_0 (mg/L) is the initial concentration of heavy metal ions, C_t (mg/L) is the corresponding concentration at different time t, V (L) is the volume of the solution, and m (g) represents the weight of soil minerals.

2.3 Adsorption isotherms and kinetics analysis

To get deeper insight into the adsorption mechanism of the effects of EDTA-2Na on the interactive behavior between soil minerals and heavy metals, the Langmuir and Freundlich isotherm models were examined to simulate the adsorption equilibrium data acquired at various concentration ranges. The Langmuir isotherm model assumes that the monolayer adsorption takes place on adsorbents that have structurally homogeneous surfaces, on which the adsorption sites are uniform and no interaction occurs between adsorbates [33]. The Freundlich isotherm model considers that multilayer adsorption occurs on energetically heterogeneous surfaces, on which the adsorbed molecules are interactive. The linear forms of the two isotherm models are given in the following Eqs. (2) and (3) [33–34]:

Langmuir isotherm model:

$$\frac{C_e}{q_e} = \frac{1}{K_L q_m} + \frac{C_e}{q_m} \quad (2)$$

Freundlich isotherm model:

$$\log q_e = \frac{1}{n} \log C_e + \log K_F \quad (3)$$

where q_e (mg/g) and C_e (mg/L) represent the adsorption capacity and the concentration of heavy metal ions in the solution at equilibrium; q_m (mg/g) is the maximum adsorption capacity; K_L (L/mg) is the constant of the Langmuir model related to the affinity of adsorbent binding sites; K_F (L/mg) and n are Freundlich isotherm constants related to adsorption capacity and adsorption strength of the adsorbent, respectively.

Furthermore, to explore the rate and rate-controlling step of heavy metal adsorption on soil minerals, the experimental data were dealt with four different kinetic models. The pseudo-first order kinetic model tents to physical interactions and assumes that the adsorption process depends on the diffusion step; the pseudo-second order kinetic model tends to chemisorption rate-limiting step in the adsorption process which is related to the condition of active sites, and the process is controlled by chemisorption mechanisms such as electron sharing or transfer among the adsorbent; the intraparticle diffusion model is usually used to explain the kinetics of the diffusion process of substances inside a particle, and

assumes that the adsorbate diffusion rate is a rate-limiting step; and the Elovich model describes multilayer adsorption on the heterogeneous surface. Four kinetic models are expressed as following Eqs. (4), (5), (6) and (7) [4, 33–34]:

The pseudo-first order kinetic model:

$$\ln(q_e - q_t) = \ln q_e - k_1 t \quad (4)$$

The pseudo-second order kinetic model:

$$\frac{t}{q_t} = \frac{1}{k_2 q_e^2} + \frac{t}{q_e} \quad (5)$$

The intraparticle diffusion model:

$$q_t = k_i t^{0.5} + C \quad (6)$$

The Elovich model:

$$q_t = \frac{1}{\beta}\ln(\alpha\beta) + \frac{1}{\beta}\ln t \quad (7)$$

where q_t (mg/g) represents the amount of metal ions adsorbed on the adsorbents at time t (min); k_1 (min^{-1}), k_2 (g/mg·min) and k_i ($mg/g·min^{0.5}$) are the rate constants of the pseudo-first order, pseudo-second order, and intraparticle diffusion models, respectively; C (mg/g) is a constant about the boundary layer thickness; α (mg/g·min) is the initial adsorption rate; and β (g/mg) is a constant related to activation energy for chemisorption and the degree of surface coverage.

2.4 Soil mineral characterization

To investigate the changes in microscopic characteristics of soil minerals under the effects of EDTA-2Na, original soil samples were reserved before the batch adsorption experiments; and minerals were performed by vacuum freeze drying after centrifugation for use in analytical instrument tests.

The changes in crystal structure of soil minerals were determined by X-ray diffraction analysis (XRD). Specifically, the dry samples were characterized by utilizing a Bruker D8 Advanced X-ray diffractometer (Bruker Co., Germany) employing Cu Kα radiation (40 kV, 40 mA). Powdered samples were scanned in the range from 10° to 80°, with a scanning step of 0.1 s/step.

To explore the changes in functional groups of soil minerals, the fourier transform infrared (FTIR) spectra of 1% mineral samples compressed by the KBr disk method were obtained on an infrared spectrometer (Nicolet iS50, Thermo Fisher Scientific, USA) from 400 to 4000 cm^{-1} at a resolution of 4 cm^{-1} with 32 scans.

To observe the apparent morphological changes of soil minerals, scanning electron microscopy (SEM; Phenom™ ProX, Phenomscientific, Netherlands) was used to visualize the micromorphology of samples

at a voltage of 20 kV.

Additionally, the specific surface area (SSA) and porosity of the mineral particles were calculated and analyzed via Brunauer Emmett Teller (BET) method by using an automatic surface area and porosity analyzer (Gemini VII 2390, Micromeritics, USA).

3 Results And Discussion

3.1 Effects of EDTA-2Na on the adsorption of Cd(II) and Pb(II) on soil minerals

3.1.1 Adsorption behavior of soil minerals for heavy metal ions

The adsorption of Cd and Pb on soil minerals that was affected by EDTA-2Na with different concentrations has been shown in Figs. 1 and 2, respectively. Generally, when the batch experiments were implemented by using SM1 and Cd, the adsorption capacity was reduced and the mobility of Cd was improved with the EDTA concentration increasing (Fig. 1a). Specifically, as the EDTA concentration increased from 0 to 600 mg/L, the maximum q_e greatly decreased from approximately 135 to 55 mg/kg due to the chelation between EDTA and Cd ions; note that the chelation was stronger than the physical adsorption of SM1, and the formed negatively charged complexes [Cd(II)EDTA^{2-}] could not be bound by negatively charged SM surface [19, 27, 35]. However, some irregular points where q_e rose unexpectedly occurred as the EDTA concentration increased (Fig. 1a). When more EDTA-2Na was added, the mole ratio (MR = moles of HM ions / sum of moles of HM ions and EDTA) increased. The matching ratio between divalent metal ions and EDTA in complexation process was 1:1 (MR = 0.5) [36]; and thus, MR less than 0.5 meant that EDTA was excessive, while MR greater than 0.5 meant that EDTA was insufficient. As Fig. 1a showed, all irregular points appeared when MR was below 0.5, because there might be mutual suppression among excess EDTA; and MR closed to 0.5 would make HM adsorption capacity on SMs decrease more efficiently. Namely, to restore environmental pollution of 50 mg/L Cd, it would be better to choose EDTA-2Na solution with a concentration of 200 mg/L, instead of 50, 400, or 600 mg/L; because the MR here was 0.45, closer to 0.5, and this remediation method was efficient and economic, even though using 400 mg/L EDTA-2Na reduced q_e by extra 4 mg/kg (Fig. 1a).

Compared with quartz sands (SM1), mineral mixtures (SM2) had a stronger adsorption capacity for HMs because they can form HM-mineral complexes via functional groups of clay [19, 37], which means a larger value range (Fig. 1a and b). Note that the HM-mineral complexes were still not as strong as [HM(II)EDTA^{2-}] complexes [1]. Therefore, the general trend of changes in q_e under the effects of EDTA with different concentration can be better presented. When the batch experiments were carried out by using SM2 and Cd, it could be more clearly observed in Fig. 1b that q_e increased rapidly when MR was

greater than 0.5 (curves above the red dotted lines); this indicated poor efficiency and insufficient EDTA-2Na dosage. Concretely, as the curves of 600 mg/L EDTA showed, q_e merely increased by 417 mg/L (from 33 to 450 mg/L) when Cd concentration rose from 25 to 200 mg/L (MR was from 0.12 to 0.52); nevertheless, it increased by 1003 mg/L (from 450 to 1453 mg/L) when Cd concentration rose from 200 to 400 mg/L (MR was from 0.52 to 0.69), which was much more rapidly. This phenomenon was also observed in the curves of 200 and 400 mg/L EDTA, which illustrated that EDTA could reduce the adsorption capacity greatly when the dosage was sufficient. Additionally, when MR was much less than 0.5 (curves below the blue dotted lines), the gaps among these curves were small; and this indicated a poor efficiency and economic with unnecessary increase in EDTA dosage.

In terms of the adsorption capacity of SMs for Pb, it was much stronger than that for Cd beacuse Pb can compete favorably for the sorption sites in soil minerals [23]. The maximum q_e of SM1 and SM2 for Pb were 660 and 19,677 mg/L, respectively (Fig. 2a and b); while that for Cd were 135 and 2,660 mg/L. Under the effects of EDTA-2Na, they decreased to 306, 19,262, 55 and 1,453 mg/L, respectively; this reconfirmed that EDTA could reduce the adsorption capacity of SMs and improve the mobility of HMs. As Fig. 2a showed, when the MR was much less than 0.5 (curves below the blue dotted lines), differences among these curves were small; when the MR was much greater than 0.5 (curves above the red dotted lines), q_e largely increased. This was in accord with the effects of EDTA with different concentrations on the adsorption capacity for Cd, and it might be generalized to most divalent metal ions. Obviously, the gap between curves of 0 and 400 mg/L EDTA was larger when MR of the point in curve of 400 mg/L was closer to 0.5 (black dotted line □ and □ were longer than □ and □, Fig. 2a). This phenomenon could also be found in the comparison between the curves of EDTA concentration equal to 0 and others. Similarly, Fig. 2b supported this law, for example, black dotted line □ was longer than □. This was because MR closer to 0.5 reduced the adsorption capacity better, making the function of EDTA-2Na more effective. Naturally, to optimally investigate the effects of other factors, such as contact time, initial pH, LMWOAs, and exogenous metal ions, on the HM-SM-EDTA system, the concentration of Cd, Pb, and EDTA-2Na were fixed as 200, 300, and 400 mg/L because it has been confirmed that this setup could make the system have a reasonable adsorption capacity and make MR close to 0.5. Additionally, mineral mixtures (SM2) had a stronger adsorption capacity for heavy metals [19], which means a larger value range and can better show the law of effects of other factors on this system; and it is more meaningful to explore the effects on mineral mixtures which are reactive and representative. Therefore, SM2 will be focused on after session 3.1.

3.1.2 Isothermal adsorption

The obtained correlation coefficients for Langmuir and Freundlich isotherm models were listed in Table 1. It can be concluded that the Langmuir model fits better with the experimental adsorption equilibrium data of both SM1 and SM2 when there was no EDTA-2Na in the system, because R^2 of the Langmuir isotherm model (> 0.97) was greater than that of the Freundlich isotherm model (> 0.90). Hence, the adsorption behaviors of both SM1 and SM2 for Cd and Pb ions suggested a monomolecular layer adsorption [4], and

the surfaces of quartz sands and mineral mixtures were structurally homogenous; there was no interaction taking place between Cd or Pb ions. By contrast, with the effects of EDTA, correlation coefficients of both isotherm models for HM adsorption on SMs mostly decreased; and it seems that the experimental data was not well in line with both isotherm models. This indicated that the introduce of EDTA-2Na destroyed the uniformity of the surfaces of mineral particles.

However, compared with the Langmuir isotherm model, the adsorption capacity (q_e) calculated from the Freundlich isotherm model were closer to the experiment value, which can be found in Fig. 3; and its correlation coefficient were also better, especially, when the MR of more points in a certain line was closer to 0.5. Specifically, when EDTA concentrations were 400 and 600 mg/L, R^2 of the Freundlich isotherm model for Cd adsorption on SM2 were even better than R^2 of non-EDTA system (0.98 and 0.94, > 0.91); Good correlation coefficients could also be found in R^2 of the Freundlich isotherm model for Pb adsorption on SM1, when EDTA concentrations were 150 mg/L (MR of more points were closer to 0.5). Therefore, under the effects of EDTA, the adsorption behaviors of both SM1 and SM2 for Cd and Pb conformed to the Langmuir isotherm model and it should be considered as a multilayer adsorption which occurred on energetically heterogeneous surfaces. In detail, on the one hand, some EDTA introduced into the HM-SM system could be adsorbed on and cover the surfaces of SMs [33, 38]; and this made the surfaces of SMs heterogeneous, blocking some adsorption sites and making them nonuniform [16, 27]. On the other hand, EDTA and HM ions were both adsorbates for SMs, and they were interactive via chelation [26, 28, 39–40]; and this was accord with the mechanism of the Freundlich isotherm model. Additionally, because the matching ratio between divalent metal ions and EDTA in chelation process was 1:1 (MR = 0.5), which meant a more effective and stable HM-SM-EDTA system, the linear relationship was better when the MR of more points in a certain line was closer to 0.5.

Table 1

Langmuir and Freundlich adsorption correlation coefficients (R^2) of SMs for Cd and Pb under the effects EDTA with different concentrations

R^2		Quartz sand (SM1)		Mineral mixture(SM2)	
Metal ion	EDTA concentration (mg/L)	Langmuir	Freundlich	Langmuir	Freundlich
Cd	0	0.9986	0.9127	0.9907	0.9087
	50	0.9610	0.8617	0.0301	0.8050
	200	0.8296	0.7795	0.5782	0.9167
	400	0.3971	0.5597	0.8987	0.9762
	600	0.2522	0.2419	0.8138	0.9430
Pb	0	0.9783	0.9691	0.9719	0.7863
	50	0.0364	0.9479	0.0520	0.5706
	150	0.0465	0.9636	0.1193	0.7050
	300	0.0109	0.9354	0.0477	0.4915
	400	0.3452	0.8587	0.0327	0.5104

3.1.3 Adsorption Kinetics

The effects of contact time on HM adsorption by SM2 were shown in Fig. 4. In the system without EDTA, it can be observed that adsorption was fast initially, then decelerated, and finally reached equilibrium (Fig. 4a). Pb adsorption onto SM2 was more rapidly than Cd, and it reached equilibrium earlier, having a higher adsorption capacity. This is because SM2 has a better affinity and selectivity towards Pb [23]. By contrast, in the system with EDTA, obvious turning points occurred in the curves (Fig. 4b). As far as Pb, faster adsorption rate made it reach a high q_t value closed to the maximum adsorption capacity, which indicated that the effect of EDTA appeared slower at the beginning. However, an abrupt turning at approximately 5 min made q_t rapidly decrease from 2.85 to 1.03 mg/g in approximately 30 min, and finally decrease to an equilibrium of 0.29 mg/g. For Cd, the turning point appeared at approximately 60 min, which was much later than Pb; and the range of the change in q_t were smaller, reaching 0.63 mg/g finally. Therefore, the contact time of 360 min was sufficient to reach equilibrium for both Cd and Pb adsorption onto SM2, and it took 5 to 10 min for EDTA to begin taking its effect. It can also be concluded that EDTA affected Pb adsorption mainly by rapidly desorbing ions after they had been adsorbed on SM, via forming very stable negatively charged complexes [Pb(II)$EDTA^{2-}$] which could not be bound by negatively charged SM surface [19, 27, 35]; while EDTA might hinder the process of Cd adsorption onto SM, via blocking the adsorption sites and chelating Cd ions simultaneously [16, 27].

Furthermore, the adsorption parameters calculated by fitting the four kinetic models are listed in Table 2. It can be observed that with and without EDTA in the system greatly affected the fitting correlation coefficients of these models for different HM ions. Nevertheless, as the Fig. 5 showed, the experimental adsorption data more in line with the pseudo-second order kinetic model than other three kinetic models; and the correlation coefficient (R^2) values of the pseudo-second order kinetic model were all greater than 0.96 (without EDTA, $R^2 > 0.99$; with EDTA, $R^2 > 0.96$). Additionally, the calculated value of q_e from the pseudo-second order kinetic model was closer to the adsorption capacity obtained from experiments than other models. Namely, the behaviors of HM adsorption onto SMs with and without the effects of EDTA were both conform to the pseudo-second order kinetic model, and the adsorption sites on SMs might be the rate-limiting step [4]. When EDTA was added, it would block the adsorption sites on SM surfaces and affect the electron transfer between adsorbents, so that the adsorption process was controlled; this still related to chemisorption rate-limiting step and obeyed the pseudo-second order kinetic model. However, R^2 decreased in the complicated HM-SM-EDTA system, because adsorption of SMs and chelation of EDTA for HMs both existed, which increased the uncertainty.

Table 2

Pseudo-first order, pseudo-second order, intraparticle diffusion and the Elovich kinetic model parameters

Kinetic models	Parameters	Analytes			
		Pb	Cd	Pb + EDTA	Cd + EDTA
Pseudo-first-order	$q_{e,exp}$ (mg g^{-1})	3.13	2.09	0.28	0.62
	$q_{e,cal}$ (mg g^{-1})	0.13	1.05	-	-
	k_1 (min^{-1})	0.0115	0.0147	-	-
	R^2	0.5361	0.9348	-	-
Pseudo-second-order	$q_{e,exp}$ (mg g^{-1})	3.13	2.09	0.28	0.62
	$q_{e,cal}$ (mg g^{-1})	3.13	2.15	0.29	0.65
	k_2 (g mg^{-1} min^{-1})	0.5593	0.0409	-0.1778	-0.0986
	R^2	1.0000	0.9990	0.9749	0.9657
Intraparticle diffusion	k_i (mg g^{-1} $min^{-0.5}$)	0.0271	0.0874	-0.1471	-0.0020
	C (mg g^{-1})	2.7630	0.7734	2.4494	0.9633
	R^2	0.4522	0.8087	0.6746	0.0019
Elovich	α (mg g^{-1} min^{-1})	2.0194×10^8	-0.0016	0.8241	1.2489×10^6
	β (g mg^{-1})	8.3195	-1.8008	3.0506	21.6450
	R^2	0.7671	0.8280	0.979	0.0908

3.2 Effects of initial pH on the system

Solution pH is another important operational parameter determining the efficiency of reducing the adsorption capacity of SMs and improving the mobility of HMs by using EDTA, so that more HM pollution can be removed from soil and groundwater system. Significantly, solution pH can affect both the speciation of HM ions and the protonation of the functional groups of SMs [41]. Generally, as pH increased, the adsorption capacity of both Cd and Pb onto SMs presented a significant increasing trend (Fig. 6). As far as Cd ions, the adsorption capacity of SM1 and SM2 was much smaller at pH < 5.5 and

4.0, respectively (Fig. 6a and b). This might be attributed to a competitive adsorption between H^+ and Cd^{2+} ions in the system and the protonation of oxide-type functional groups (> SiOH, >AlOH, >Al_2OH, >AlSiOH) on SM2 [20, 33, 42]; and the low pH had a weaker effect on SM2 than SM1 because SM2 had a stronger initial adsorption capacity and more active sites for H^+ and Cd^{2+} ions to compete [21]. In terms of Pb, though the adsorption capacity was also smaller at low pH, it was much higher than Cd in the range of 4.0–7.0; this was because the potential selectivity of SMs for Pb ions was preferential [33]. Additionally, the adsorption capacity greatly increased at pH > 7.0 due to the formation of metal hydroxide precipitates for Cd and Pb ions, and these precipitates cannot combine with or be break by EDTA [43]. Cd ions began to speciate to $CdOH^+$, $Cd(OH)_2$ and $Cd(OH_3)^-$ later than Pb, so adsorption capacity for Cd started to obviously increased at a higher pH than Pb.

Furthermore, it was observed that the adsorption capacity of Cd and Pb maintained a low level at pH below 7.0 and 4.0, respectively; and then increased sharply (Fig. 6). This indicated that EDTA had strong chelating ability for Cd and Pb ions, and could improve mobility of HMs and reduce adsorption capacity of SMs at a relatively wide pH range; while this range for Cd was wider. Notably, the optimal pH for EDTA to take effects in Cd-SM1, Pb-SM1, Cd-SM2, and Pb-SM2 system was around 4.0, 4.0, 4.0 and 3.0, respectively.

3.3 Effects of exogenous chemicals on the system

To simulate the effects of exogenous chemicals which commonly exist in the natural environment on the system, low-molecular-weight organic acids (LMWOAs) and exogenous metal ions served as the important factors. Low-molecular-weight organic acids (LMWOAs) are hydrophilic acids with some special characteristics, such as reducibility, COOH/OH-richness, and complexation with metal ions [44–47]; besides, it has some resemblances with EDTA and is abundant in the environment. Therefore, it is significant to investigate effects of LMWOAs on the system, when it works with EDTA (humic acid has similar characteristics and was involved). As Fig. 7 showed, in the non-EDTA system, the adsorption capacity of both Cd and Pb onto SM2 mostly changes little under the effects of LMWOAs except citric and humic acids. Because most LMWOAs did not have a strong chelating ability like EDTA to desorb metal ions, and cannot reduce the adsorption capacity independently. As far as HM-SM-EDTA system, the extent of changes in adsorption capacity depended on the types of LMWOAs and HMs (Fig. 7). For Cd ions, there was decrease in the adsorption capacity under the effects of acetic, crtric, malonic, succinic and tartaric acids, while there was increase under the effects of ascorbic, humic and oxalic acids; however, the changes were all not obvious because the adsorption performance of Cd itself is not as good as Pb that can compete favorably for the sorption sites in oxides and the clay fraction [23]. Therefore, changes in the adsorption capacity of Pb were analyzed to explore the mechanism of the effects of LMWOAs.

It can be obviously observed that tartaric and acetic acids made the adsorption capacity greatly increase from 924 mg/kg to 1623 and 2455 mg/kg (by 699 and 1531 mg/kg), respectively. Notably, tartaric acid has two carboxyl groups and one hydroxyl group; acetic acid contains a carboxyl group. They could bridge Pb ions and SM2 surface sites via these functional groups by forming the bridging (LMWOA-Pb-SM2), so that some Pb ions avoided chelating with EDTA and were adsorbed onto SM2; tartaric acid had

more functional groups and larger molecular weight than acetic acid, resulting in better bridge ability [45, 48]. Additionally, complexation of COOH/OH-rich LMWOAs and surface hydroxyls on SM2 via ligand exchange reactions could increase negative charges on SM2 surfaces, which made SM2 have a stronger ability to adsorb Pb ions [47, 49–50].

Furthermore, the results showed that ascorbic, malonic, oxalic and succinic acid reduced the Pb adsorption capacity of SM2 from 924 mg/kg to 584, 752, 769 and 547 mg/kg. Here are the mechanisms. Firstly, ascorbic and oxalic acids have reducibility, and the combination of them with EDTA probably reduced the adsorption by improving the reductive dissolution of oxide-type functional groups on SM2 surface, which could strongly bind Pb ions [46, 51]. Secondly, oxalic, succinic and malonic acids could form complexes with Pb ions via their carboxyl and hydroxyl groups, performing effects similar to EDTA and promoting adsorption reduction. Thirdly, these LMWOAs all had a relatively high adsorption affinity towards SM2 by the interaction among their COOH/OH groups and oxide-type groups of SM2 (> SiOH, >AlOH), resulting in the LMWOA adsorption onto SM2, like the effects of EDTA; this performance would compete for adsorption sites with Pb ions, enhance the mobility of Pb ions, and reduce the adsorption capacity of SM2 [44, 49, 52]. In summary, LMWOAs affected the system mainly by bridging, complexation, adsorption site competition and reductive dissolution; and the extent might depend on the synthesis of diverse effects.

Heavy metal ions usually coexisted with other metal ions in the soil and groundwater environment, so it is significant to investigate the effects of exogenous metal ions on the HM-SM-EDTA system. As Fig. 8 showed, there were nearly no change in the system without EDTA, which illustrated that it was difficult for exogenous metal ions to greatly affect the Cd and Pb adsorption capacity of SM2 before it reached adsorption saturation; and SM2 had a relatively strong ability of adsorption, so the competition between metal ions for active sites on SM2 could ignored. By contrast, in the HM-SM-EDTA system, there was increase in the Cd and Pb adsorption capacity onto SM2. Specifically, Cu^{2+}, Fe^{2+} and Pb^{2+} ions increased the Cd adsorption capacity following the sequence: Cu > Pb > Fe; and that of Pb was Cu > Cd > Fe. Note that EDTA had different selectivity for different metal ions, and there was competition between cations for complexation with EDTA [46, 53]. The uptake selectivity here was Cu > Pb (Cd) > Fe, resulting in the effects on the mobility of the target HMs and the adsorption capacity of SMs. Additionally, it could be seen that Al^{3+} and Cr^{3+} ions affected the system little, because EDTA generally had a stronger complexation with divalent metal ions than trivalent metal ions.

3.4 Characterization of soil minerals affected by EDTA-2Na

3.4.1 FTIR analysis

To investigate the changes in functional groups of soil minerals, the FTIR spectra of soil mineral mixtures (SM2) with and without the effects EDTA was shown in Fig. 9. For mineral mixtures, the absorbance at 461–471 cm^{-1} was attributed to O-Si-O bending vibrations, the absorbance at 914–920 cm^{-1} was attributed to Al-OH-Al formation, and the peak at 1041 cm^{-1} was attributed to Fe-O bending vibrations, which revealed that the original sample consisted of mixed composites of Si, Al, and Fe oxides; this confirmed the abovementioned oxide-type groups on SM2 surface. The bands at 3551, 3474 and 3415 cm^{-1} were attributed to structural OH groups of clay minerals. After introducing EDTA, the stronger

characteristic absorption band appearing at 1400 cm^{-1} and new peak at 1100 cm^{-1} could be assigned to C-O stretching vibration of the -COO^- group, which were functional groups of EDTA. Changes in the peak position and intensity at 468 cm^{-1} indicated the dissolution of Metal-Si oxides. The carboxylic OH peak around 3626 cm^{-1} and the weakened bands at 2919, 2850, 2426 cm^{-1} confirmed the attachment of EDTA onto SM2.

3.4.2 XRD analysis

The changes in crystal structure of soil minerals determined by XRD analysis were presented in Fig. 10. The results showed that the diffraction peaks of quartz, illite and montmorillonite used in this study were a match with the standard diffraction peaks of quartz (JCPDS No. 85–0798), illite (JCPDS No. 26–0911) and montmorillonite (JCPDS No. 29-1498); thus, the three components of the mineral mixture (SM2) had high purity and could be used for the investigation. The characteristic diffraction peaks appearing in mineral mixtures with and without the effects of EDTA had both been marked using Q, I, M which means quartz, illite and montmorillonite, respectively. The peak intensity generally decreased under the effect of EDTA, suggesting that EDTA molecules were attached on the surface of mineral particles. A peak at approximately 2θ = 66° disappeared under the effect of EDTA, maybe because the dissolution of Metal-Si oxides [46], which was also confirmed by FTIR analysis.

3.4.3 Morphology of the soil minerals

Morphology of the SM2 samples was observed by the SEM to investigate the apparent changes of soil minerals. Figure 11a presented the micrograph of mineral mixtures without the effects of EDTA. Note that the wettability and swelling of clay (illite and montmorillonite) in the mineral mixture would occur when it interacted with water [22]. Besides a large particle, there were many microparticles in Fig. 11a1 and a2; obviously, many small cracks, concavities and convexities appeared on the surface of some particles, which made mineral particles rougher (Fig. 11a3). These were all attributed to the clay swelling and dispersion after being soaked in water (solution without EDTA) [43]. It could be clearly observed from Fig. 11b that mineral particles changed a lot under the effects of EDTA, during the batch adsorption experiments. Firstly, many tiny white substances appeared on the soil minerals (Fig. 11b1 and b2), which might be the attached EDTA. Secondly, there were many microparticles adhering to large particles due to the enhanced adhesion of minerals under the effects of EDTA (Fig. 11b2 and b3), which filled many pores; whereas the surfaces of particles in Fig. 11a1 and a3 were clean. Thirdly, particles agglomerated (Fig. 11b4), and connected with each other by something like fiber bands because of the attachment of EDTA (Fig. 11b5); while particles were independent in Fig. 11a2. Additionally, it could be seen that EDTA also made particles smoother, clogging the active sites on mineral surfaces and reducing its adsorption for HMs [27]. This is in accord with the observation reported by a previous study (Fig. 11b1) [16]. Overall, all changes including attachment of EDTA and microparticles, agglomeration, connection and the smoother surfaces contributed to reducing specific surface areas and adsorption capability of SM2.

3.4.4 BET analysis

Table 3 showed the changes in the BET specific surface areas (SSA), pore size and the pore volume of SM2 under the effects of EDTA. Concretely, as EDTA concentration increased from 0 to 600 mg/L, the SSA gradually decreased from 16.73 to 12.59 m^2/g, and the micropore area decreased from 2.03 to

0.09 m^2/g. It decreased more at the low EDTA concentration (50 and 200 mg/L), while external surface area decreased more at the high EDTA concentration (400 and 600 mg/L); this indicated that EDTA might block the micropore area and made the surface smoother first, then played a role in promoting the attachment of microparticles, agglomeration and connection, which could reduce the external surface area. Additionally, there were decrease in the pore volume and pore size under the effects of EDTA, which illustrated that EDTA molecules attached to SM2 surface and narrowed the pore volume. This confirmed to the observation in SEM analysis, and coincided with results presented by Ren et al. [33] and Repo et al. [41].

Table 3

BET analysis of SM2 samples under the effects of EDTA with different concentrations

Samples			BET Surface Area (m^2/g)	Micropore Area (m^2/g)	External Surface Area (m^2/g)	Pore Volume (cm^3/g)	Pore Size (nm)	Method
Soil	Metal ion	EDTA (mg/L)						
Mineral mixture (SM2)	Cd	0	16.7283	2.0319	14.6964	0.039664	8.5141	N_2
		50	14.6663	0.5271	14.1392	0.037049	8.21345	N_2
		200	14.4732	0.1664	14.3068	0.036763	8.21765	N_2
		400	12.5995	0.0937	12.5058	0.034746	8.1539	N_2
		600	12.5865	0.0443	12.5422	0.034473	8.1319	N_2

4 Conclusions

In this study, effects of EDTA-2Na on adsorption of Cd(II) and Pb(II) by SMs were explored, and the changes in microscopic characteristics of SMs were also determined by diverse instrument analysis to investigate the mechanisms. Results showed that EDTA could reduce the HM adsorption capacity of SMs effectively and economically at a reasonable MR value, which was around 0.5. Note that the contact time had a great impact on the effect of EDTA in terms of Pb. As for as other factors, the optimal initial pH for EDTA to take effects in Cd-SM1, Pb-SM1, Cd-SM2, and Pb-SM2 system was approximately 4.0, 4.0, 4.0 and 3.0, respectively; the extent of the effects of LMWOAs on the HM-SM-EDTA system depended on the synthesis of bridging, complexation, adsorption site competition and reductive dissolution; while that of exogenous metal ions was decided by the selectivity of EDTA to them. Significantly, changes in functional groups, the attachment of EDTA onto SMs and the decrease in SSA of SMs were observed, indicating that EDTA reduced the HM adsorption capacity of SMs not only by complexation with HM ions, but also decreasing SSA and blocking active sites. Hence, the above results can advance the remediation technology of soil and groundwater pollution, especially pump-and-treat remediation.

Abbreviations

EDTA:ethylenediaminetetraacetic acid; HM:heavy metal; SM:soil mineral; MR:mole ratio; LMWOAs:low-molecular-weight organic acids; XRD:X-ray diffraction; FTIR:fourier transform infrared; SSA:specific surface area; BET:Brunauer Emmett Teller; SEM:scanning electron microscopy.

Declarations

Authors' contributions

XY designed and performed all experiments, analyzed the data and was a major contributor to writing the manuscript. SL and CD were major contributors to supervision, guided the batch adsorption experiments and contributed to writing the manuscript. GZ and YD contributed to supervision, administrative issues regarding the experiments. YG, ANM, JTAJ, YT and KHL are important contributors to supervision. All authors read and approved the final manuscript.

Author details

[1] Department of Hydraulic Engineering, College of Civil Engineering, Tongji University, 1239 Siping Road, Shanghai 200092, China. [2] The Yangtze River Water Environment Key Laboratory of the Ministry of Education, Tongji University, 1239 Siping Road, Shanghai 200092, China. [3] School of Environmental and Geographical Sciences, Shanghai Normal University, No. 100 Guilin Road, Shanghai 200234, China. [4] Department of Civil Engineering, McMaster University, 1280 Main Street West, Hamilton, ON L8S4L7, Canada. [5] Institute of Water and Ecology Problems, Far East Branch of the Russian Academy of Sciences, Khabarovsk, Russia. [6] Department of Civil and Environmental Engineering, Pontifical Catholic University of Rio de Janeiro, Rio de Janeiro, Brazil. [7] Department of Environmental Engineering, Faculty of Engineering and Green Technology, Universiti Tunku Abdul Rahman, 31900 Kampar, Perak, Malaysia.

Acknowledgments

Not applicable.

Funding

This research is financially supported by the National Natural Science Foundation of China (41672230, 41601514, 51961145106), Shanghai science and technology innovation action plan project (19ZR1459300,19230742400), the Interdisciplinarity Fund of Peak Discipline from Shanghai Municipal Education Commission (0200121005/053, 2019010202), Key Laboratory of Yangtze River Water Environment for Ministry of Education, Tongji University (YRWEF201604), State Key Laboratory of Petroleum Pollution Control (PPC2016019), and the International Exchange Program for Graduate Students, Tongji University (No. 201902053).

Ethics approval and consent to participate

Not applicable.

Consent for publication

Not applicable.

Availability of data and materials

The data used and analyzed during this study are available from the corresponding author on reasonable request.

Competing interests

The authors declare that they have no competing interests.

References

1. Zhang S, Wen J, Hu Y, Fang Y, Zhang H, Xing L, Wang Y, Zeng G (2019) Humic substances from green waste compost: An effective washing agent for heavy metal (Cd, Ni) removal from contaminated sediments. J Hazard Mater 366:210-218
2. Wen X, Lu J, Wu J, Lin Y, Luo Y (2019) Influence of coastal groundwater salinization on the distribution and risks of heavy metals. Sci Total Environ 652:267-277
3. Bandow N, Simon F (2016) Significance of cadmium from artists' paints to agricultural soil and the food chain. Environ Sci Eur 28(12)
4. Pu S, Hou Y, Yan C, Ma H, Huang H, Shi Q, Mandal S, Diao Z, Chu W (2018) In Situ Coprecipitation Formed Highly Water-Dispersible Magnetic Chitosan Nanopowder for Removal of Heavy Metals and Its Adsorption Mechanism. Acs Sustain Chem Eng 6(12):16754-16765
5. Jamali MK, Kazi TG, Arain MB, Afridi HI, Jalbani N, Memon AR, Shah A (2007) Heavy metals from soil and domestic sewage sludge and their transfer to Sorghum plants. Environ Chem Lett 5(4):209-218
6. Sahito OM, Afridi HI, Kazi TG, Baig JA (2015) Evaluation of heavy metal bioavailability in soil amended with poultry manure using single and BCR sequential extractions. Int J Environ An Ch 95(11):1066-1079
7. Repo E, Warchol JK, Bhatnagar A, Sillanpaa M (2011) Heavy metals adsorption by novel EDTA-modified chitosan-silica hybrid materials. J Colloid Interface Sci 358(1):261-267
8. Bai J, Chao Y, Chen Y, Wang S, Qiu R (2019) The effect of interaction between Bacillus subtilis DBM and soil minerals on Cu(II) and Pb(II) adsorption. J Environ Sci-China 78:328-337
9. Kazi TG, Wadhwa SK, Afridi HI, Talpur FN, Tuzen M, Baig JA (2015) Comparison of essential and toxic elements in esophagus, lung, mouth and urinary bladder male cancer patients with related to controls. Environ Sci Pollut R 22(10):7705-7715
10. Zhang RK, Wang P, Lu YC, Lang L, Wang L, Lee SC (2019) Cadmium induces cell centrosome amplification via reactive oxygen species as well as endoplasmic reticulum stress pathway. J Cell Physiol 234(10):18230-18248
11. Zeng G, He Y, Zhan Y, Zhang L, Pan Y, Zhang C, Yu Z (2016) Novel polyvinylidene fluoride nanofiltration membrane blended with functionalized halloysite nanotubes for dye and heavy metal ions removal. J Hazard Mater 317:60-72

12. Fu F, Wang Q (2011) Removal of heavy metal ions from wastewaters: A review. J Environ Manage 92(3):407-418
13. Mahmoud A, Hoadley AFA (2012) An evaluation of a hybrid ion exchange electrodialysis process in the recovery of heavy metals from simulated dilute industrial wastewater. Water Res 46(10):3364-3376
14. Li Z, Alessi D, Zhang P, Bowman RS (2002) Organo-Illite as a Low Permeability Sorbent to Retard Migration of Anionic Contaminants. J Environ Eng 128(7):583-587
15. Liu C, Ball WP (2002) Back diffusion of chlorinated solvent contaminants from a natural aquitard to a remediated aquifer under well-controlled field conditions: Predictions and measurements. Groundwater 40(2):175-184
16. You X, Liu S, Dai C, Zhong G, Duan Y, Tu Y (2019) Acceleration and centralization of a back-diffusion process: Effects of EDTA-2Na on cadmium migration in high- and low-permeability systems. Sci Total Environ:135708. doi: 10.1016/j.scitotenv.2019.135708
17. Yan S, Liu Y, Liu C, Shi L, Shang J, Shan H, Zachara J, Fredrickson J, Kennedy D, Resch CT, Thompson C, Fansler S (2016) Nitrate bioreduction in redox-variable low permeability sediments. Sci Total Environ 539:185-195
18. Chapman SW, Parker BL (2005) Plume persistence due to aquitard back diffusion following dense nonaqueous phase liquid source removal or isolation. Water Resour Res 41(12):12411-12426
19. Zhang C, Liu X, Lu X, Meijer EJ, Wang K, He M, Wang R (2016) Cadmium(II) Complexes Adsorbed on Clay Edge Surfaces: Insight From First Principles Molecular Dynamics Simulation. Clay Clay Miner 64(4):337-347
20. Tournassat C, Davis JA, Chiaberge C, Grangeon S, Bourg IC (2016) Modeling the Acid-Base Properties of Montmorillonite Edge Surfaces. Environ Sci Technol 50(24):13436-13445
21. Zhang C, Liu X, Lu X, He M, Jan Meijer E, Wang R (2017) Surface complexation of heavy metal cations on clay edges: insights from first principles molecular dynamics simulation of Ni(II). Geochim Cosmochim Ac 203:54-68
22. Mészáros R, Jobbik A, Varga G, Bárány S (2019) Electrosurface properties of Na-bentonite particles in electrolytes and surfactants solution. Appl Clay Sci 178:105127
23. Cerqueira B, Vega FA, Serra C, Silva LFO, Andrade ML (2011) Time of flight secondary ion mass spectrometry and high-resolution transmission electron microscopy/energy dispersive spectroscopy: A preliminary study of the distribution of Cu2+ and Cu2+/Pb2+ on a Bt horizon surfaces. J Hazard Mater 195:422-431
24. Wanner P, Parker BL, Hunkeler D (2018) Assessing the effect of chlorinated hydrocarbon degradation in aquitards on plume persistence due to back-diffusion. Sci Total Environ 633:1602-1612
25. Duo L, Yin L, Zhang C, Zhao S (2019) Ecotoxicological responses of the earthworm Eisenia fetida to EDTA addition under turfgrass growing conditions. Chemosphere 220:56-60
26. Gonzalez-Estrella J, Li G, Neely SE, Puyol D, Sierra-Alvarez R, Field JA (2017) Elemental copper nanoparticle toxicity to anaerobic ammonium oxidation and the influence of ethylene diamine-tetra

acetic acid (EDTA) on copper toxicity. Chemosphere 184:730-737

27. Tõnsuaadu K, Viipsi K, Trikkel A (2008) EDTA impact on Cd2+ migration in apatite–water system. J Hazard Mater 154(1-3):491-497
28. Guo X, Zhao G, Zhang G, He Q, Wei Z, Zheng W, Qian T, Wu Q (2018) Effect of mixed chelators of EDTA, GLDA, and citric acid on bioavailability of residual heavy metals in soils and soil properties. Chemosphere 209:776-782
29. Shahid M, Pinelli E, Dumat C (2012) Review of Pb availability and toxicity to plants in relation with metal speciation; role of synthetic and natural organic ligands. J Hazard Mater 219:1-12
30. Parker BL, Chapman SW, Guilbeault MA (2008) Plume persistence caused by back diffusion from thin clay layers in a sand aquifer following TCE source-zone hydraulic isolation. J Contam Hydrol 102(1-2):86-104
31. Ball WP, Liu C, Xia G, Young DF (1997) A diffusion-based interpretation of tetrachloroethene and trichloroethene concentration profiles in a groundwater aquitard. Water Resour Res 33(12):2741-2757
32. Ayral-Cinar D, Demond AH (2017) Effective diffusion coefficients of DNAPL waste components in saturated low permeability soil materials. J Contam Hydrol 207:1-7
33. Ren Y, Abbood HA, He F, Peng H, Huang K (2013) Magnetic EDTA-modified chitosan/SiO2/Fe3O4 adsorbent: Preparation, characterization, and application in heavy metal adsorption. Chem Eng J 226:300-311
34. Fallah Z, Isfahani HN, Tajbakhsh M (2019) Cyclodextrin-triazole-titanium based nanocomposite: Preparation, characterization and adsorption behavior investigation. Process Saf Environ 124:251-265
35. Mosai AK, Tutu H (2019) The effect of crop exudates and EDTA on cadmium adsorption by agricultural podsolic soil: implications on groundwater. Int J Environ Sci Te 16(7):3071-3080
36. Karak T, Paul RK, Das DK, Boruah RK (2016) Complexation of DTPA and EDTA with Cd2+: stability constants and thermodynamic parameters at the soil-water interface. Environ Monit Assess 188(12)
37. Chen W, Lei T, Lv W, Hu Y, Yan Y, Jiao Y, He W, Li Z, Yan C, Xiong J (2018) Atomic Interlamellar Ion Path in High Sulfur Content Lithium-Montmorillonite Host Enables High-Rate and Stable Lithium-Sulfur Battery. Adv Mater 30(40):1804084
38. Mahmoudian M, Nozad E, Hosseinzadeh M (2018) Characterization of EDTA Functionalized Graphene Oxide/Polyethersulfone (FGO/PES) Nanocomposite Membrane and Using for Elimination of Heavy Metal and Dye Contaminations. Polymer Korea 42(3):434-445
39. Kim EJ, Jeon E, Baek K (2016) Role of reducing agent in extraction of arsenic and heavy metals from soils by use of EDTA. Chemosphere 152:274-283
40. Kent DB, Davis JA, Joye JL, Curtis GP (2008) Influence of variable chemical conditions on EDTA-enhanced transport of metal ions in mildly acidic groundwater. Environ Pollut 153(1):44-52

41. Repo E, Warchol JK, Kurniawan TA, Sillanpaa MET (2010) Adsorption of Co(II) and Ni(II) by EDTA- and/or DTPA-modified chitosan: Kinetic and equilibrium modeling. Chem Eng J 161(1-2):73-82
42. Zarzycki P, Thomas F (2006) Theoretical study of the acid-base properties of the montmorillonite/electrolyte interface: Influence of the surface heterogeneity and ionic strength on the potentiometric titration curves. J Colloid Interf Sci 302(2):547-559
43. Altin O, Ozbelge OH, Dogu T (1999) Effect of pH, flow rate and concentration on the sorption of Pb and Cd on montmorillonite: I. Experimental. Journal of Chemical Technology & Biotechnology 74(12):1131-1138
44. Fang D, Wei S, Xu Y, Xiong J, Tan W (2019) Impact of low-molecular weight organic acids on selenite immobilization by goethite: Understanding a competitive-synergistic coupling effect and speciation transformation. Sci Total Environ 684:694-704
45. Chen J, Lu T, Wang Y, Li J, Fu X, Qi Z, Zhang Q (2019) Transport of graphene oxide nanoparticles in saturated kaolinite- and goethite-coated sand columns: effects of low-molecular-weight organic acids. Environ Sci Pollut R 26(24):24922-24932
46. Wei M, Chen J, Wang Q (2018) Remediation of sandy soil contaminated by heavy metals with Na2 EDTA washing enhanced with organic reducing agents: element distribution and spectroscopic analysis. Eur J Soil Sci 69(4):719-731
47. Dinh QT, Li Z, Tran TAT, Wang D, Liang D (2017) Role of organic acids on the bioavailability of selenium in soil: A review. Chemosphere 184:618-635
48. Huang L, Hu H, Li X, Li LY (2010) Influences of low molar mass organic acids on the adsorption of Cd2+ and Pb2+ by goethite and montmorillonite. Appl Clay Sci 49(3):281-287
49. Favorito JE, Eick MJ, Grossl PR (2018) Adsorption of Selenite and Selenate on Ferrihydrite in the Presence and Absence of Dissolved Organic Carbon. J Environ Qual 47(1):147-155
50. Wu H, Jiang D, Cai P, Rong X, Huang Q (2011) Effects of low-molecular-weight organic ligands and phosphate on adsorption of Pseudomonas putida by clay minerals and iron oxide. Colloids Surf B 82(1):147-151
51. Yu B, Jia S, Liu Y, Wu S, Han X (2013) Mobilization and re-adsorption of arsenate on ferrihydrite and hematite in the presence of oxalate. J Hazard Mater 262:701-708
52. Wijnja H, Schulthess CP (2000) Interaction of Carbonate and Organic Anions with Sulfate and Selenate Adsorption on an Aluminum Oxide. Soil Sci Soc Am J 64(3):898
53. Turgut C, Katie Pepe M, Cutright TJ (2004) The effect of EDTA and citric acid on phytoremediation of Cd, Cr, and Ni from soil using Helianthus annuus. Environ Pollut 131(1):147-154

Figures

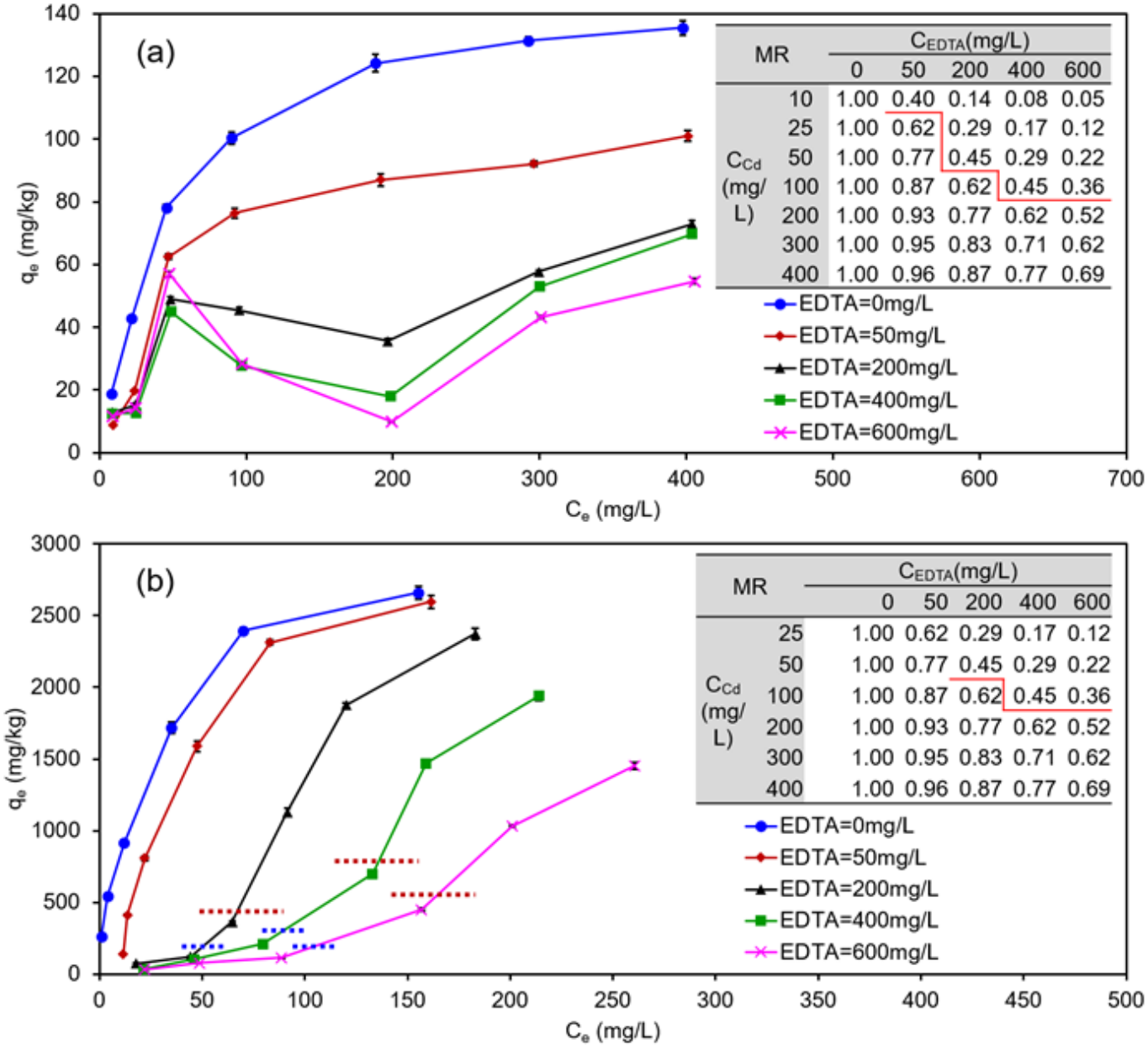

Figure 1

Effects of concentration of EDTA on the Cd(II) adsorption capacity of (a) SM1, and (b) SM2. All error bars represent standard deviation from triplicate experiments. When not shown, error bars are smaller than symbols.

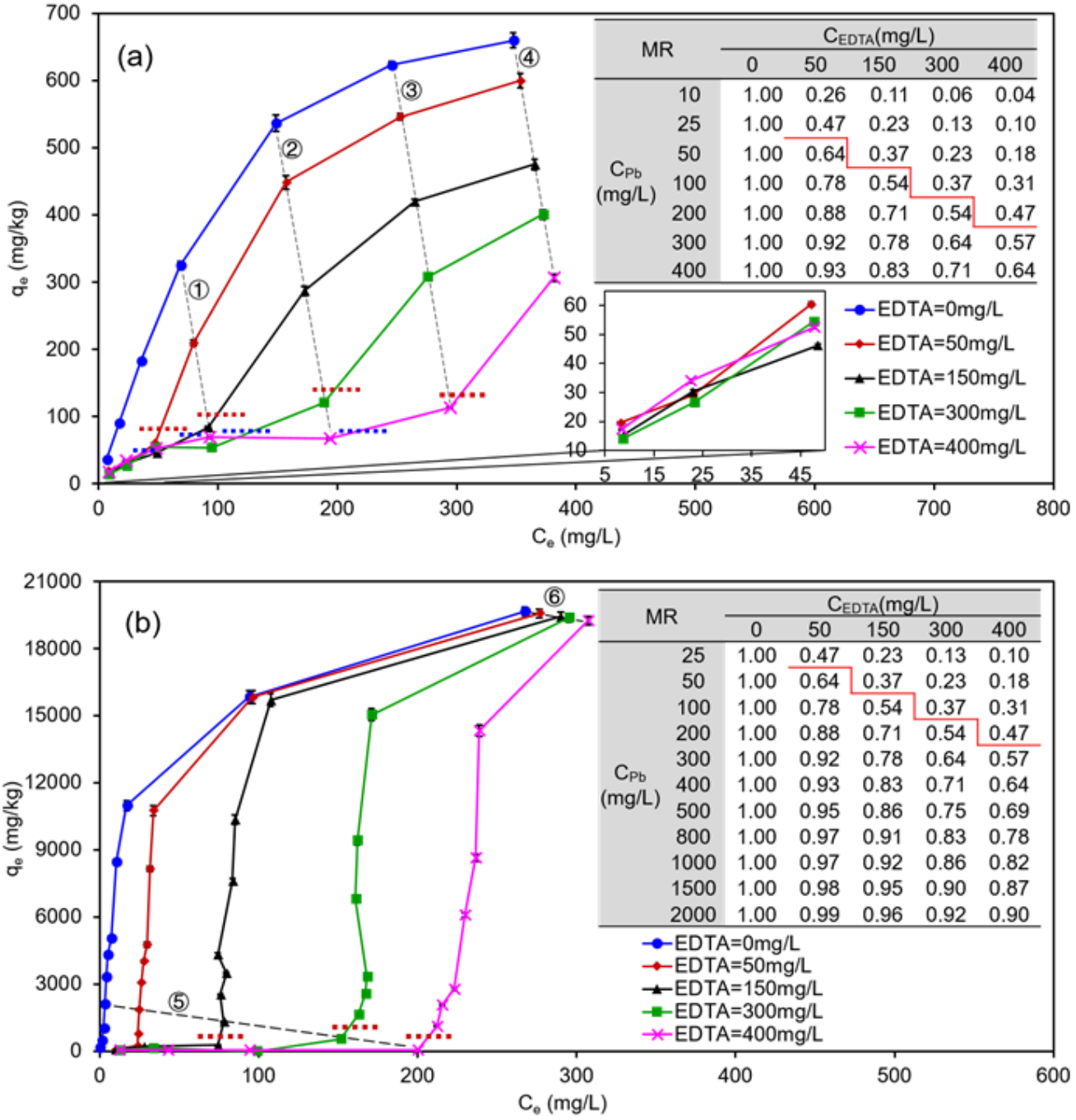

Figure 2

Effects of concentration of EDTA on the Pb(II) adsorption capacity of (a) SM1, and (b) SM2. All error bars represent standard deviation from triplicate experiments. When not shown, error bars are smaller than symbols.

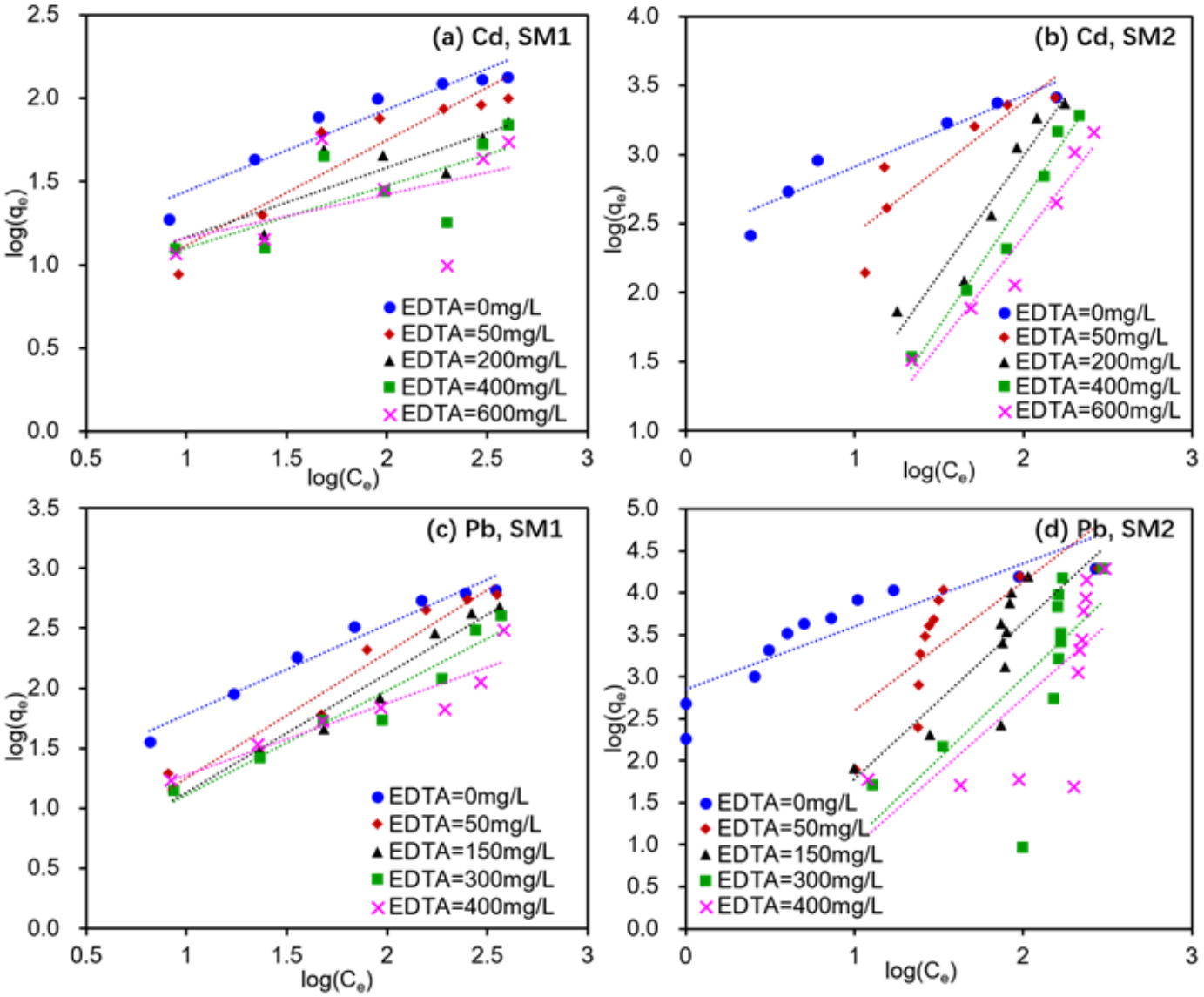

Figure 3

Freundlich isotherm model for Cd(II) adsorption on (a) SM1, and (b) SM2; and Freundlich isotherm model for Pb(II) adsorption on (c) SM1, and (d) SM2.

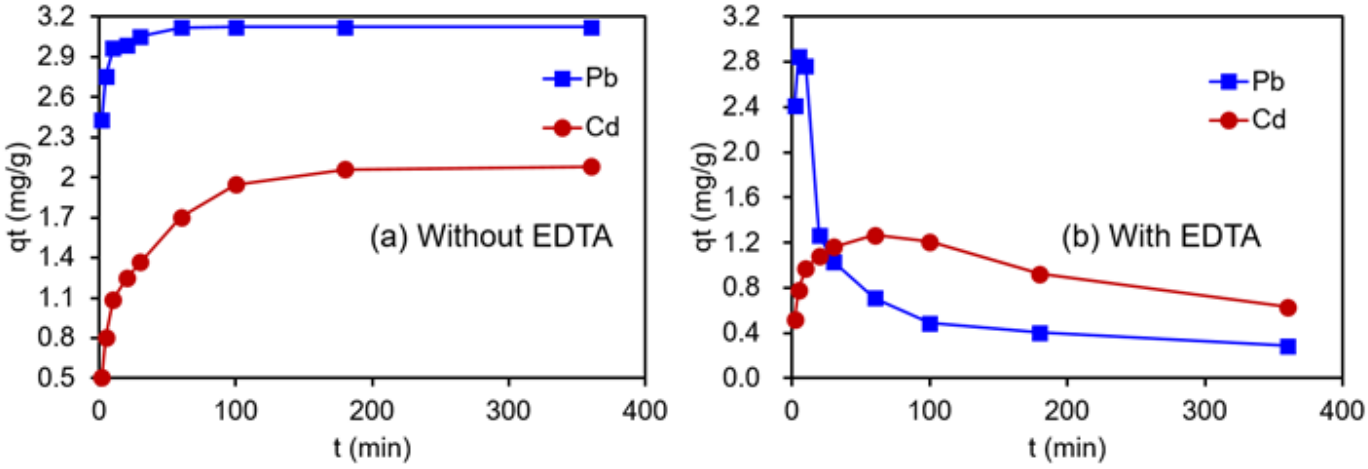

Figure 4

Effects of contact time on the adsorption of HM ions by SM2, (a) without the effect of EDTA, and (b) with the effect of EDTA

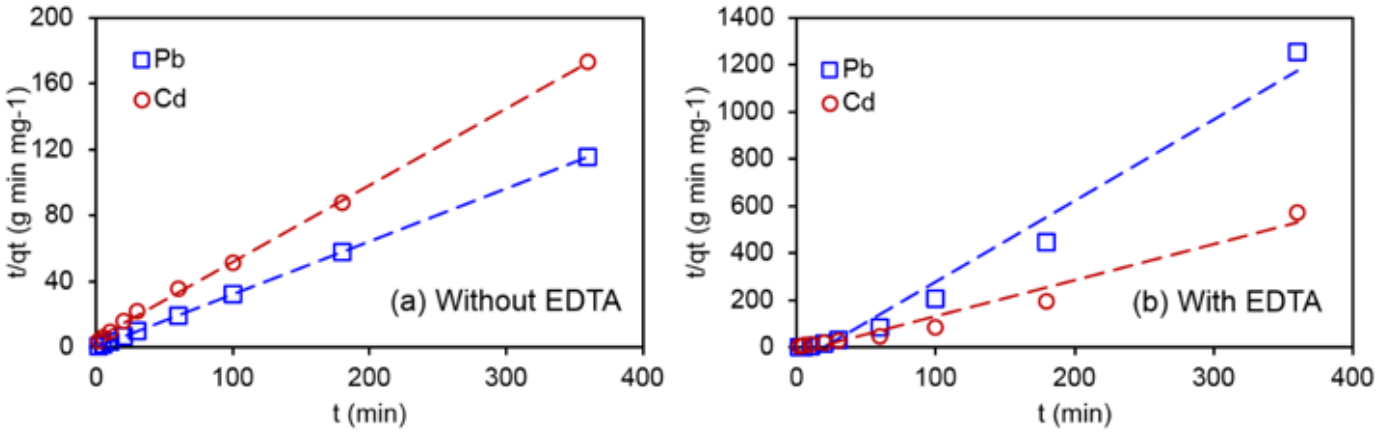

Figure 5

Pseudo-second order kinetic model plots for the adsorption of HM ions onto SM2, (a) without the effect of EDTA, and (b) with the effect of EDTA

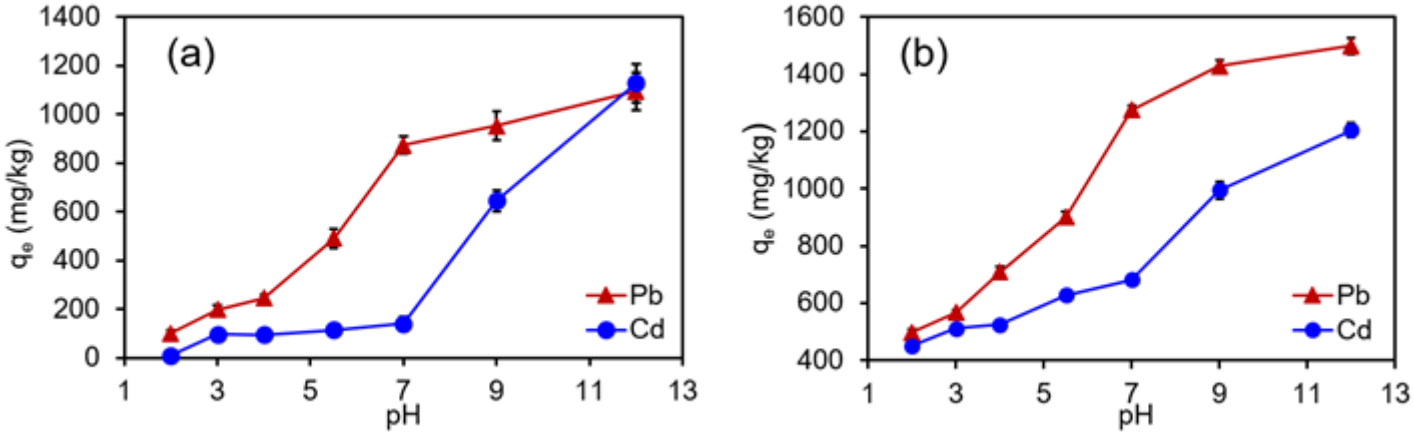

Figure 6

The effects of initial pH on the HM-SM-EDTA system, low-permeability soil minerals:(a) SM1, (b) SM2. All error bars represent standard deviation from triplicate experiments. When not shown, error bars are smaller than symbols.

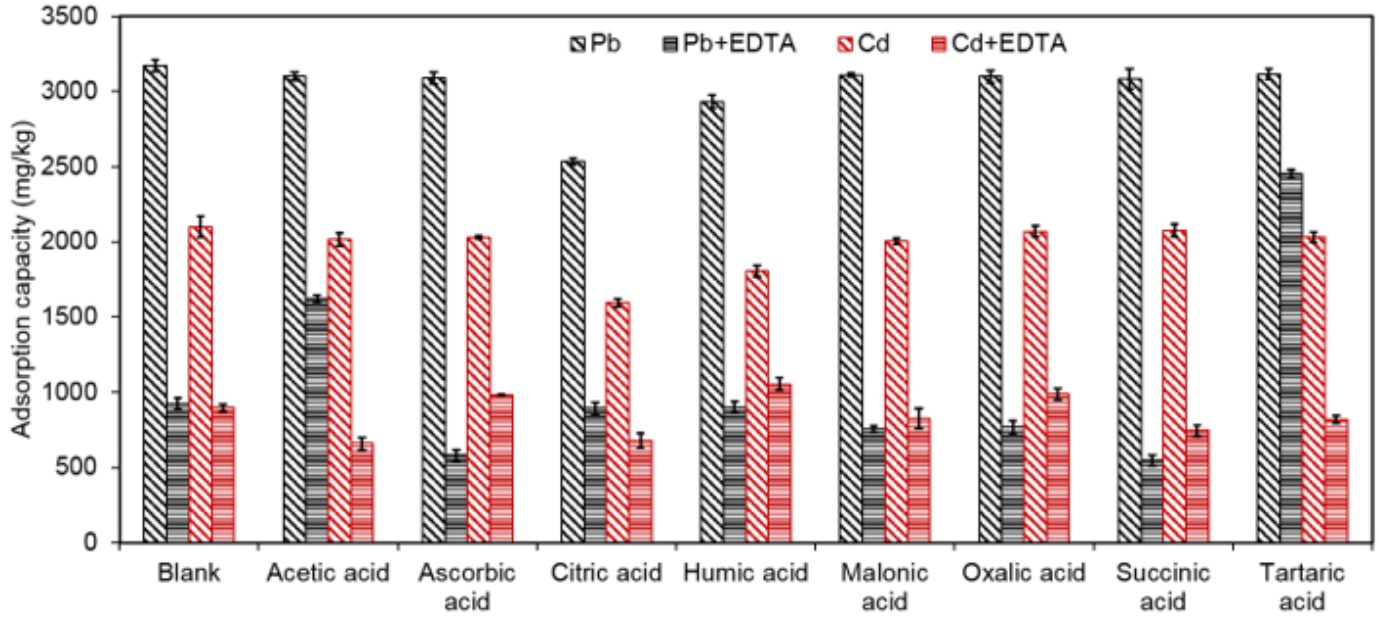

Figure 7

Effects of low-molecular-weight organic acids on the HM-SM-EDTA system, the low-permeability soil mineral was SM2. All error bars represent standard deviation from triplicate experiments.

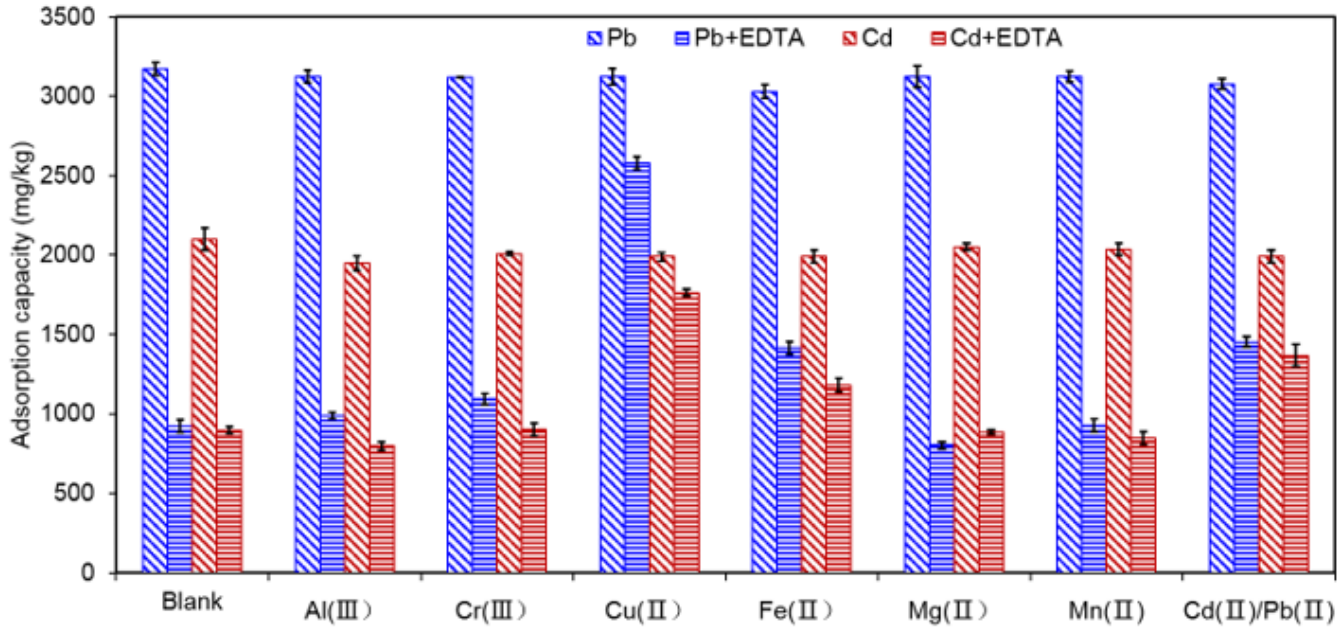

Figure 8

Effects of exogenous metal ions on the HM-SM-EDTA system, the low-permeability soil mineral was SM2. All error bars represent standard deviation from triplicate experiments.

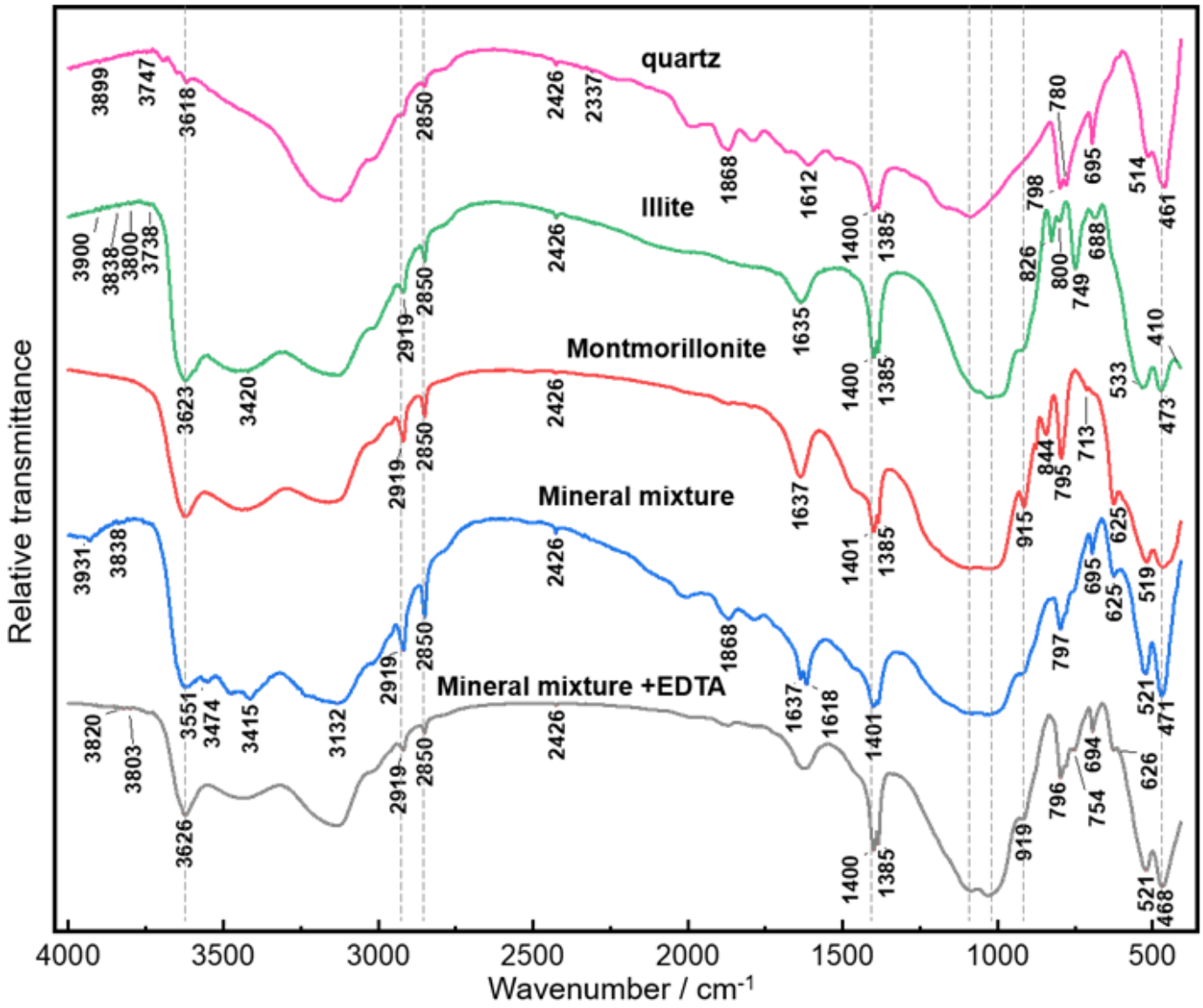

Figure 9

FTIR spectra of the mineral mixture (SM2) with and without the effects of EDTA, and the components of SM2 (quartz, illite and montmorillonite)

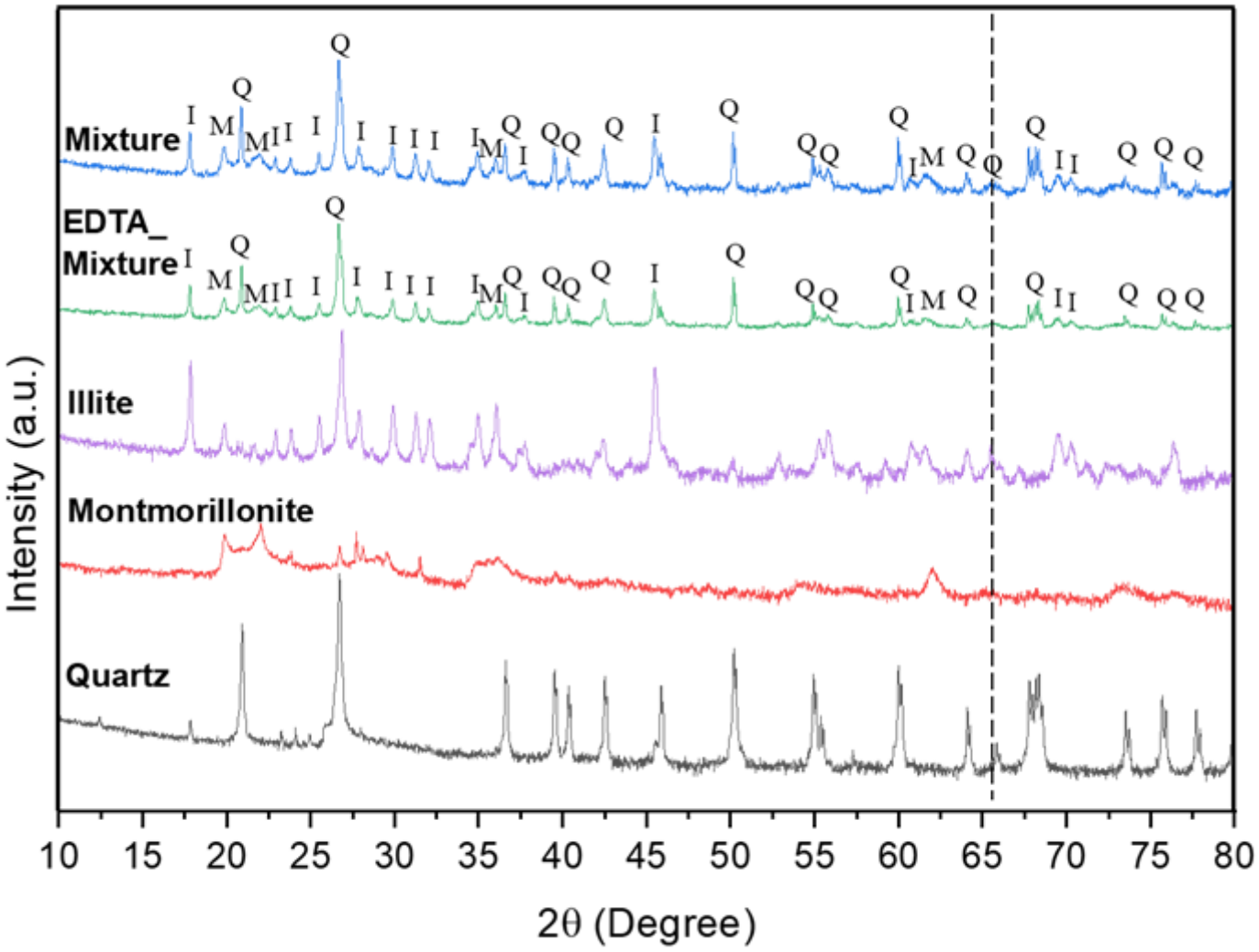

Figure 10

XRD patterns of the mineral mixture (SM2) with and without the effects of EDTA, and the components of SM2 (quartz, illite and montmorillonite); Q, I, M represents characteristic diffraction peaks from quartz, illite and montmorillonite, respectively

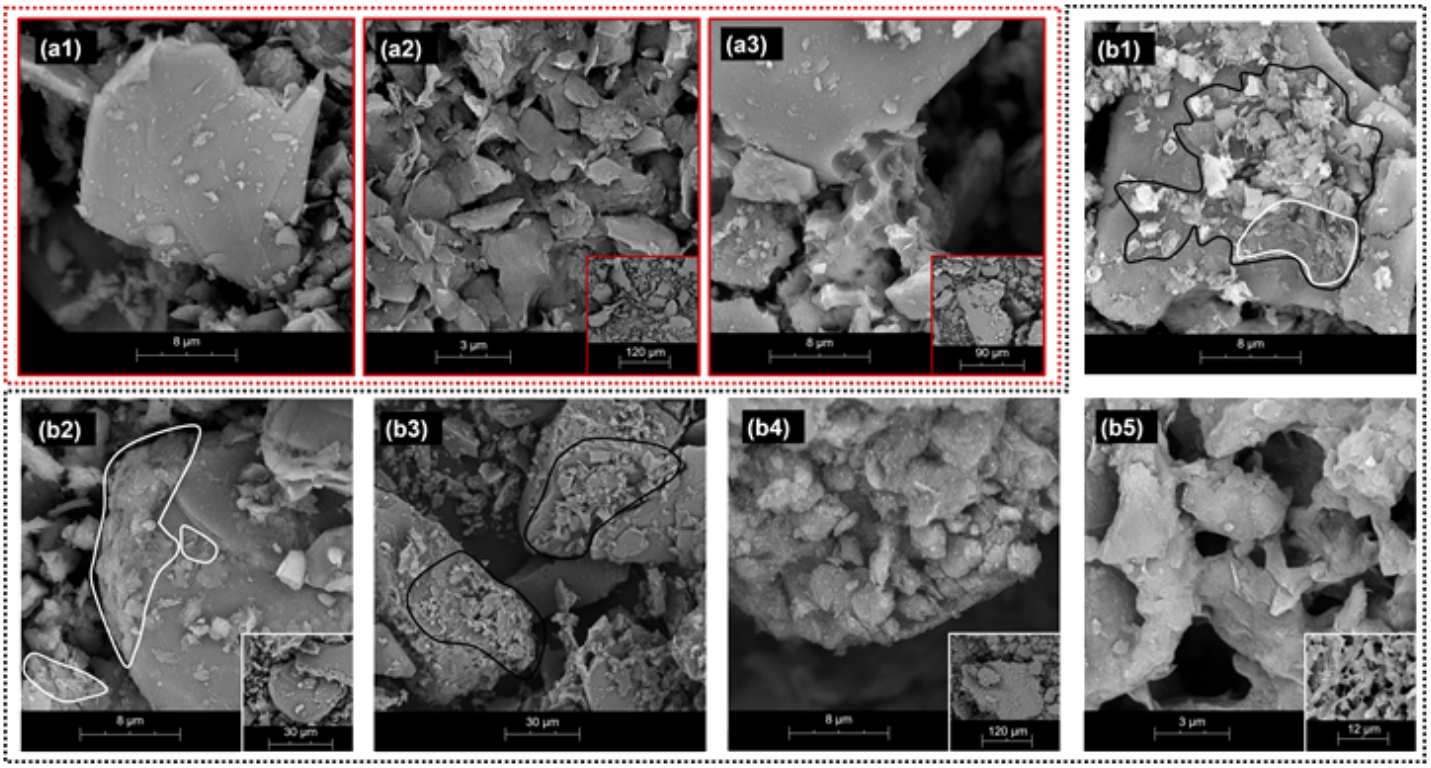

Figure 11

Scanning electron microscopy images of SM2 (mineral mixture) particles before and after adsorption experiments, without and with the effect of EDTA: (a1) large particles, (a2) independent particles and (a3) cracks, concavities and convexities on particles without the effect of EDTA; (b2) and (b3) were the attachment of EDTA and microparticles, in accord with findings of previous studies (b1) [16]; (b4) agglomeration and (b5) connection with the effect of EDTA